# Impacts of the closure of the Mozambique Channel on the southwest Indian Ocean circulation: A regional numerical simulation

Théo Le Hir [a,b,*], Pierrick Penven [a], Thierry Huck [a],*, Romain Pellen [b], Maryline Moulin [b], Marina Rabineau [b], Daniel Aslanian [b]

[a] Univ Brest, CNRS, Ifremer, IRD, Laboratoire d'Océanographie Physique et Spatiale (LOPS), IUEM, Technopôle Brest Iroise, rue Dumont d'Urville, Plouzané, 29280, France
[b] Univ Brest, CNRS, Ifremer, UBS, Geo-Ocean, IUEM, Technopôle Brest Iroise, rue Dumont d'Urville, Plouzané, 29280, France

## ARTICLE INFO

## ABSTRACT

Paleobathymetric reconstructions suggest that 35 million years ago, local uplift of the Davie Ridge could have temporarily raised a continental land–bridge between Africa and Madagascar and dramatically affected their connectivity. Numerical simulations of a regional model of the southwest Indian Ocean at mesoscale resolution are performed to investigate the consequences of such a closure of the Mozambique Channel. Compared to a reference simulation of present day circulation, blocking the Mozambique Channel results in a redistribution of the transport around Madagascar dramatically strengthening the East Madagascar Current and eddy variability south of Madagascar, broadening the Agulhas Current, and modifying water mass properties and bottom circulation.

## 1. Introduction

Madagascar is home to one of the most unusual, endemic, diverse, and endangered concentrations of wildlife in the world. To explain its unique and unbalanced biological diversity, Simpson (1940) proposed the "sweepstakes hypothesis", according to which the ancestors of mammals present in Madagascar today arrived from Africa by raft. This theory is important in biogeographical and evolutionary terms explaining how animals colonize new frontiers, but its validity is currently under debate (McCall, 1997; Mazza et al., 2019; Masters et al., 2021; Génin et al., 2022; Lopes et al., 2023). The cross-sectional study of the Cenozoıc biogeography of Madagascar and the geodynamic results obtained from a large dataset within the framework of the PAMELA project (Lopes et al., 2023; Pellen et al., 2022) concluded that several phases of regional uplift during the Cenozoıc affected connectivity between Africa and Madagascar. These uplift phases led to the modern topography of Madagascar (Masters et al., 2021), separated today from Africa by 450 km of deep basin. A recent reconstruction of the paleobathymetry of the Mozambique Channel region during one of these phases which occurred between 36 and 30 million years ago (Pellen et al., 2022) shows the Davie Ridge forming a continental bridge between Mozambique and the south of Madagascar (Fig. 1), as suggested earlier by McCall (1997).

Nowadays, oceanic circulation in the southwest Indian Ocean is dominated by waters of the westward flowing South Equatorial Current (SEC) (Tomczak and Godfrey, 1994). When reaching the east coast of Madagascar around 17°S, the SEC splits into two opposite branches (Fig. 2): the North Madagascar Current (NMC) flowing to the North and the East Madagascar Current (EMC) flowing to the South (Chapman et al., 2003). On reaching the African coast at 11°S, the NMC also splits into two. The northward branch feeds the East African Coastal Current (EACC) (Chapman et al., 2003). The southward branch flows through the Mozambique Channel, generating large Mozambique channel rings propagating southward and dominating circulation in the channel (Schott and McCreary, 2001). Although it shows large variations, a mean southward transport of 16.7 Sv (1 Sv = $10^6$ m$^3$ s$^{-1}$) has been reported for the 2003–2008 period (van der Werf et al., 2010; Ridderinkhof et al., 2010). Along the south and west coasts of Madagascar, the EMC forms a western boundary current transporting about 20 Sv towards the pole (Ponsoni et al., 2016; Voldsund et al., 2017).

At the southern mouth of the Mozambique Channel, outflows from both the channel and the EMC merge to feed the Agulhas Current along the east coast of South Africa (Lutjeharms, 2006). At the southwestern tip of the Agulhas Bank, the Agulhas Current retroflects to flow

---

* Corresponding authors.
  *E-mail addresses:* theo.lehir@univ-brest.fr (T. Le Hir), thuck@univ-brest.fr (T. Huck).
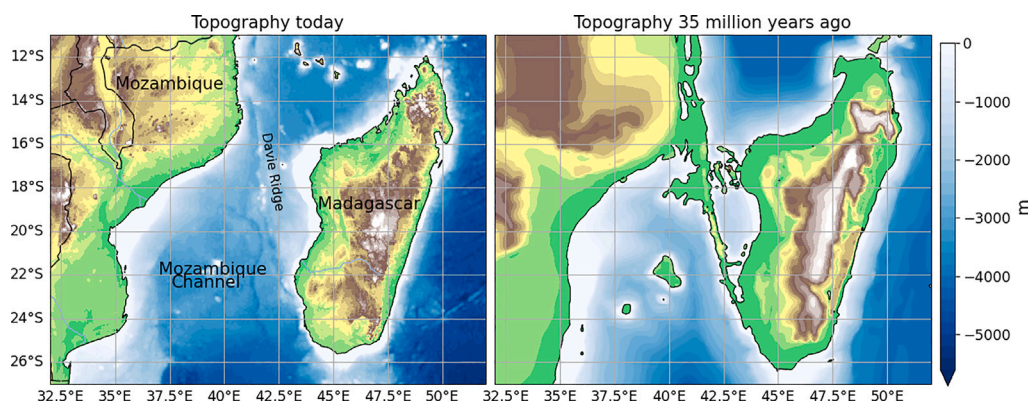
**Fig. 1.** Topography of the Mozambique Channel for the present day (Weatherall et al., 2015) (a), and for 35 million years ago (b), according to a recent reconstruction of the Digital Terrain Model based on a treatment of the regional uplift affecting Davie Ridge (Pellen et al., 2022).

eastwards to form the Agulhas Return Current (ARC) (Lutjeharms and Ansorge, 2001) (Fig. 2). Fifteen Sv of Agulhas waters leaks into the South Atlantic, feeding the returning branch of the global thermohaline circulation (Richardson, 2007). This Agulhas leakage from the Indian to the Atlantic Ocean has been recognized as critical for Atlantic meridional overturning circulation, influencing global Earth climate (Beal et al., 2011).

As bottom topography controls the south western Indian oceanic circulation with local and larger scale consequences (Speich et al., 2006; Penven et al., 2006), it might be asked how bathymeric changes associated with past uplift phases in the Mozambique channel would affect the structure of the greater Agulhas current system. Here, we investigate with a numerical model how the ocean circulation in and around the Mozambique Channel may have changed in response to past bathymetric modifications. By removing Madagascar in a realistic numerical ocean model simulation, Penven et al. (2006) have shown it enables the formation of a regular western boundary current in the Mozambique Channel extending continuously down the Agulhas. On the contrary, is interesting, from a geophysical fluid dynamics point of view, to investigate how the ocean circulation would react to the closure of the Mozambique Channel, as the whole South Indian Ocean western boundary current would have to flow along the east coast of Madagascar, and how this would affect the Agulhas current.

As a first step towards regional paleocurrent reconstruction, this study addressed the sensitivity of oceanic circulation and mesoscale turbulence to changes in bottom topography in current conditions. It consists in numerically simulating the southwest Indian Ocean in a present-day (1993–2018) regional ocean model configuration at a 1/12° resolution to resolve mesoscale eddies. After a comparison with in-situ and satellite observations, we launched a new configuration (called TOPO-BRIDGE hereafter) with the bathymetry of the Mozambique Channel modified to as it was 35 million years ago, when the Mozambique Channel was closed. We then addressed the impact of such a topographic change on the circulation, eddy dynamics and the evolution of water masses in the region. Blocking the Mozambique Channel results in a redistribution of the transport around Madagascar dramatically strengthening the EMC and eddy variability south of Madagascar, broadening (but not strengthening) the Agulhas Current, and modifying water mass properties and bottom currents in the region.

After a presentation of the numerical experiments and a comparison with in-situ and satellite observations, we show the consequences of topographic changes on ocean transport, mesoscale variability, water mass properties and bottom currents.

## 2. Material and method

### 2.1. CROCO ocean model and SWAG configuration

The model employed here is the Coastal and Regional Ocean COmmunity model (CROCO, https://www.croco-ocean.org/) (Auclair et al.,

2022). CROCO is an evolution of Regional Ocean Modeling Systems (ROMS), a regional primitive equation model based on topography following vertical grid and higher order numerical schemes (Shchepetkin and McWilliams, 2005). As CROCO is able to address oceanic flows, eddies, and their interplay with topography at coastal scale while resolving their interactions with larger scales, it is suitable for the representation of turbulent dynamics in the southwest Indian Ocean (Tedesco et al., 2019).

The SouthWest indiAn subtropical Gyre (SWAG12) configuration is a regional application of the CROCO ocean model to the greater Agulhas Current system as a whole. It uses a single grid from 2.5°W to 66°E and from 46.75°S to 4.8°S. For the present experiments, a horizontal resolution of 1/12° allows to represent the dominant processes such as the NMC, the EMC, the Agulhas current, the ARC and the mesoscale eddies in the Mozambique Channel and the Agulhas Retroflection (Fig. 2). Seventy-five s-coordinate levels guarantee the resolution of the vertical stratification. Bottom topography for the reference experiment stems from the General Bathymetric Chart of the Oceans version 2020 (GEBCO Bathymetric Compilation Group, 2020). To limit errors associated with the vertical coordinate, topography is smoothed to maintain a relative slope parameter $r = \frac{|h_{i+1} - h_{i-1}|}{h_{i+1} + h_{i-1}}$ below 0.25 (Beckmann and Haidvogel, 1993). Initial and lateral boundary conditions are derived from the GLORYS Global Ocean Physics Reanalysis at 1/12° resolution (Lellouche et al., 2018). Surface fluxes are derived using bulk formulas for heat, freshwater and momentum from hourly ERA5 atmospheric reanalysis variables (Hersbach et al., 2020). The model is run for 26 years (1993–2018) with a two year spin up.

### 2.2. Comparison with observations

We compare the results of our reference simulation (called hereafter REF) to satellite sea surface height (SSH) observations (Fig. 2) and in-situ temperature and salinity mean climatology (Fig. 3). Then we briefly describe the large-scale flows and water masses of the southwestern Indian Ocean that are of interest for our study.

Fig. 2 compares the sea surface height standard deviation (RMS SSH hereafter) for the reference experiment (REF, panel b) with AVISO altimetry data (Taburet et al., 2019, panel a). RMS SSH illustrates the surface mesoscale turbulence and mean SSH acts as a streamfunction for the mean surface geostrophic circulation. REF mean SSH contours follow the SEC and its north/south separation when approaching East Madagascar around ~17°S, the NMC, the EMC, the Agulhas current, the Agulhas Retroflection, the ARC and its standing meanders. Although slightly on the lower side, REF RMS SSH are comparable with observations with values between 15 cm and 25 cm in the Mozambique Channel and south of Madagascar (Halo et al., 2014a) and values larger than 40 cm in the Agulhas Retroflection and in the ARC.

Fig. 3 compares temperature and salinity meridional sections cutting through the Mozambique Channel at 42°S between REF and World
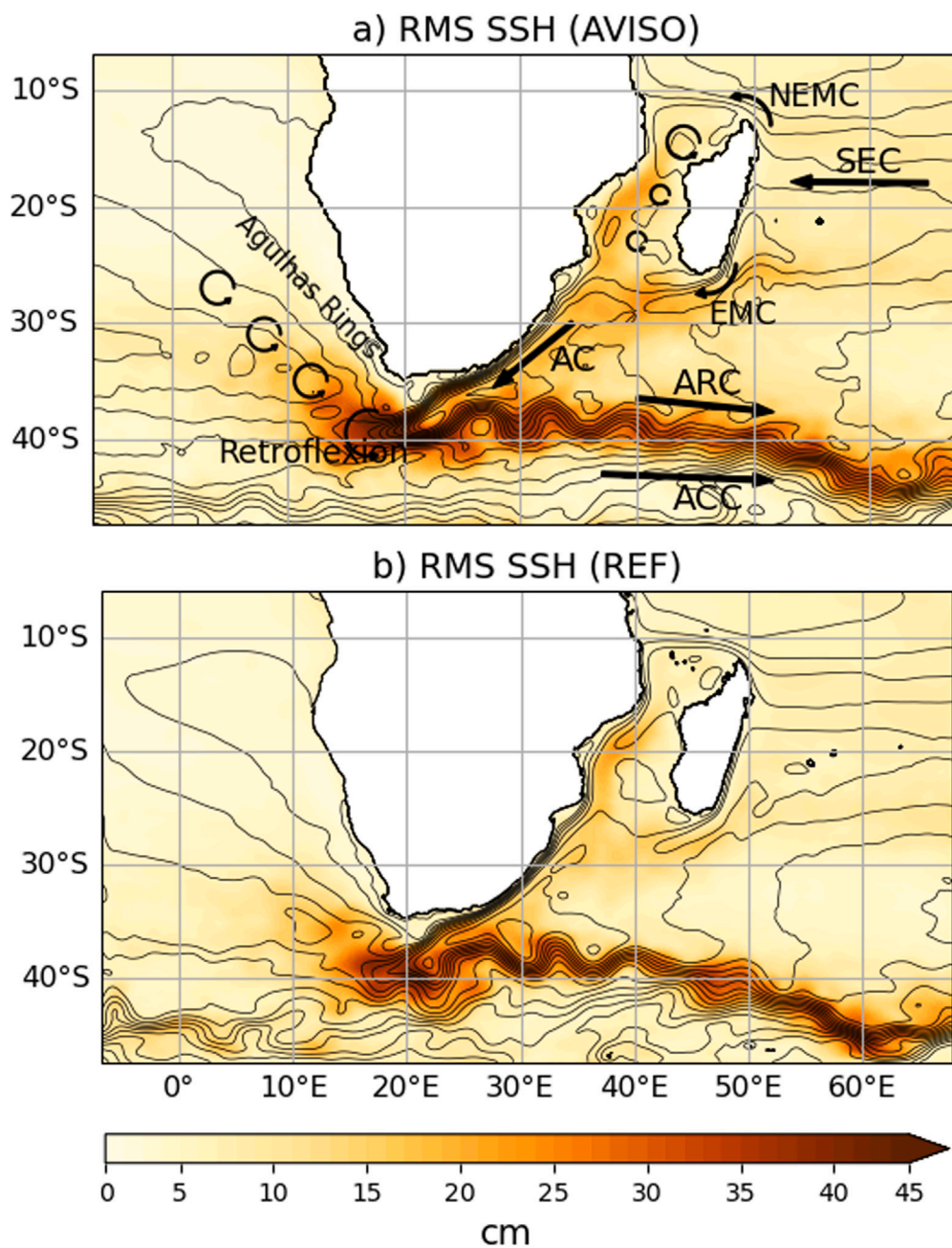
**Fig. 2.** Standard deviation of sea surface height (RMS SSH) calculated over 2008–2017 from daily mean values, for AVISO observations (a) and for the reference (REF) simulation (b) (Contour Interval 10 cm). The main currents in the area are (anticlockwise) the South Equatorial Current (SEC), the North Madagascar Current (NMC) and the East Madagascar Current (EMC), the Agulhas Current (AC), the Agulhas Return Current (ARC) and the Antarctic Circumpolar Current (ACC).

Ocean Atlas 2018 climatology (Locarnini et al., 2018, WOA2018). There is no significant difference between REF and observations for temperature (Fig. 3a,b). The model reproduces the strong thermocline in the upper ocean. The salinity sections (Fig. 3c,d) shows that modeled Tropical Surface Water (TSW) does not extend as far south in the model as in the observations. Likewise, the salinity minimum extending from the south at 1000 m depth associated with Antarctic Intermediate Water (AAIW) does not extend as far north compared with WOA2018. = However, the location of the subtropical front and its structure in temperature and salinity are well captured in the reference simulation. From the north, at a depth of about 1000 m, is the Red Sea Water (RSW), marked by high salinities (Tomczak and Godfrey, 1994). It follows the African coast until it reaches the sources of the Agulhas Current. Its signature in the simulation does not extend as far south compared to WOA. The cold and salty North Atlantic Deep Water

(NADW) formed by convection in the North Atlantic propagates at depth towards the Southern Ocean and arrives between 2500 m and 3500 m south of the Mozambique Channel. It does not appear in REF above the 34.8 salinity contour as in WOA (Fig. 3c,d) but the salinity of the whole layer remains above 34.78 (not shown). In the observations, it slightly overshoots the Davie Ridge at 20°S as suggested by Charles et al. (2020), as well as the North Indian Deep Water (NIDW) arriving from the north of the channel.

### 2.3. Idealized configuration with a modified topography

For our idealized experiment TOPO-BRIDGE, we modified the model bathymetry in the Mozambique Channel according to a recent reconstruction at 35 million years based on geodynamics and a treatment of the regional uplift affecting Davie Ridge by Pellen et al. (2022)
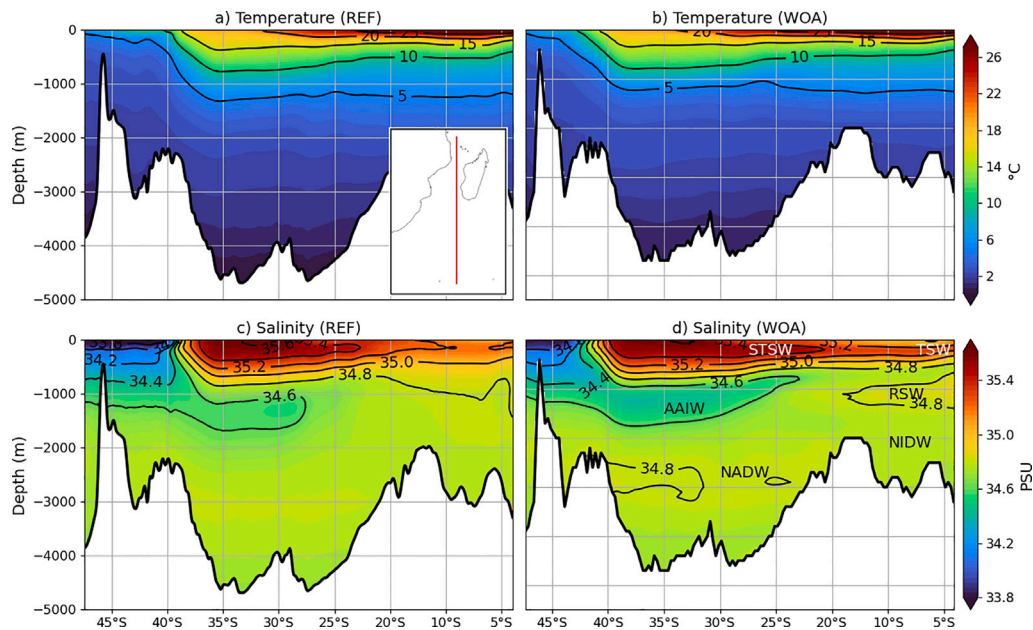
**Fig. 3.** Meridional sections of temperature (top) and salinity (bottom) averaged over 2008–2017 along the Mozambique Channel at 42°E for the reference simulation REF (right) and observations from the World Ocean Atlas (left). The following water masses are found from top to bottom: Tropical Surface Water (TSW), Subtropical Surface Water (STSW), Red Sea Water (RSW), Antarctic Intermediate Water (AAIW), North Indian Deep Water (NIDW), North Atlantic Deep Water (NADW).

(Fig. 1b). In this reconstruction, the Davie ridge emerges entirely and forms islands at several locations (22°S/40°E and 23°S/38°E).

The topography reconstruction by Pellen et al. (2022) was first interpolated on the model regular grid in the Mozambique Channel region. Fig. 4a shows the bathymetry used for REF. For a smooth transition from the original topography outside the Mozambique Channel region to the reconstruction inside, we defined a buffer zone between the two frames (see Fig. 4b) in which the bathymetry varies following $\alpha \times$ (reference bathymetry) + $(1-\alpha) \times$ (35 million year bathymetry), with $\alpha$ decreasing linearly from 1 on the outer frame of the buffer zone to 0 on the inner frame. The resulting bathymetry is smoothed to respect the relative slope parameter $r < 0.25$ criterion. We manually removed the lakes in the land-sea mask.

## 3. Results

Both simulations are kinetically adjusted before 1995. To guarantee a sufficiently long period for statistical significance to the new conditions, the statistics are calculated over the last 10 years (i.e. 2008–2017) for both simulations. In the first subsection, we present the impacts of the closure of the Mozambique Channel on the mean circulation and the mesoscale turbulence, and in the second, the resulting changes in water mass composition.

### 3.1. Mean circulation and mesoscale turbulence

The net southward transport across the Mozambique Channel was estimated at an average of 16.7 Sv from the moored LOCO (Long-term Ocean Climate Observations) current-meter array between 2004–2008 (Ridderinkhof et al., 2010), with large interannual variability. REF Mozambique transport is higher (25.7 Sv). van der Werf et al. (2010) underline discrepancies in the ability of numerical models to capture this feature. The Agulhas Current has an average flow of 77 Sv (Beal et al., 2015), fed by transport from Mozambique Channel and the EMC (Lutjeharms, 2006). The first question that comes to mind when we block the Mozambique Channel is what happens to the transport that was passing through the channel and how the general circulation in the Agulhas system is affected by this.

**Table 1**

Southward transport for the two main contributors to the Agulhas Current (AC): the Mozambique Channel and the East Madagascar Current (EMC), in the observations (Beal et al., 2011; Lutjeharms et al., 1981; Ridderinkhof et al., 2010), the reference simulation (REF) and the simulation with modified topography (TOPO-BRIDGE). For the numerical simulations, the transport is averaged over 2008–2017.

| Transport (Sv) | Mozambique | EMC | Agulhas current |
|---|---|---|---|
| Observations | 16.7 | 18.3 | 77.0 |
| REF | 25.7 | 24.6 | 82.0 |
| TOPO-BRIDGE | – | 45.6 | 100.2 |

Fig. 5 shows the average transport for each configuration. For both REF and TOPO-BRIDGE simulations, AC and EMC vertically integrated transport are computed in the same way as for the observations, using the respective sections and distances to the coast (219 km and 100 km) defined in Beal et al. (2015) and Ponsoni et al. (2016). The sections where the vertically integrated transport of the AC and EMC were measured are shown in Fig. 5. In REF, the net southward transport averaged over 2008–2017 is 25.7 Sv for the Mozambique Channel, 24.6 Sv for the EMC, and 82 Sv for the AC. These values are reasonably close to observations (Table 1). In TOPO-BRIDGE, an EMC transport increase (+21.0 Sv) almost compensates for the transport that passed through the channel in the reference simulation. The transport of the AC increases by 18.2 Sv. For each of the two model configurations, about 60 to 70 Sv in the AC originates from the EMC and the Mozambique Channel. In addition, about 20 Sv for REF and 40 Sv for TOPO-BRIDGE come from recirculations associated with increased mesoscale variability (see zooms on Fig. 5).

Table 1 summarizes these results.

The increase in EMC transport for TOPO-BRIDGE leads to the appearance of a strong barotropic cyclonic recirculation gyre (~80 Sv centered at 39°E/25°S with a radius of about 350 km) in the southwest of Madagascar. This loop in the mean transport appears to be related to a large increase in mesoscale eddy variability south of Madagascar (Fig. 6). The detachment of the southward extension of the EMC from the southern tip of Madagascar is known to generate eddy dipoles, with cyclones inshore and anticyclones offshore (de Ruijter et al., 2004). ARC transport is not significantly affected by the topography
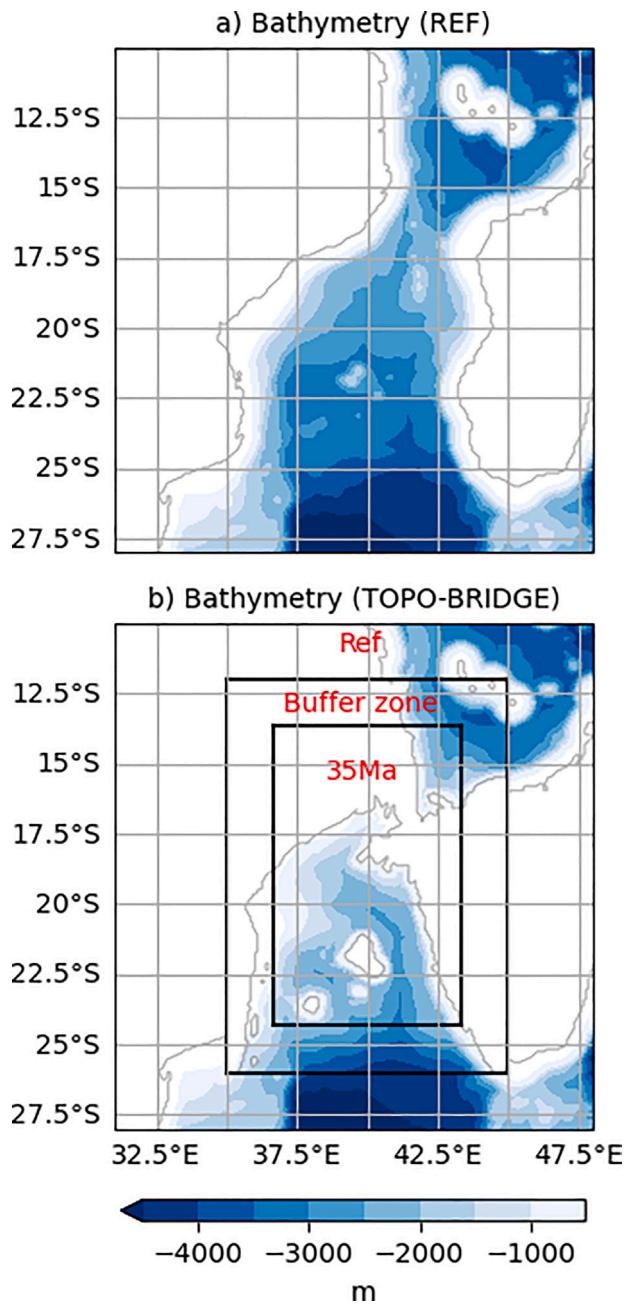
Fig. 4. Mozambique Channel bathymetry used for (a) the reference simulation REF and (b) for the simulation with the modified bathymetry TOPO-BRIDGE. The bathymetry inside the 35Ma area corresponds to the bathymetry 35 million years ago. The bathymetry inside the buffer zone area changes linearly from the 35 Ma bathymetry to the reference bathymetry outside the area.

SSH animations day by day (available as supplementary material), we notice in the TOPO-BRIDGE simulation a larger amount of cyclonic and anticyclonic eddies in the southwest of Madagascar and propagating westward towards the Agulhas Current. A larger eddy variability can actually be seen for all the southwest Indian subgyre in the TOPO-BRIDGE simulation (Fig. 6b). In contrast, TOPO-BRIDGE mesoscale eddy variability appears reduced in the core of the EMC along the Madagascar east and south coasts (Fig. 6b) and in the western part of the retroflection in the Cape Basin.

To address the changes induced by adding a bridge in the vertical structure of the AC and EMC, we calculated the mean currents orthogonal to the sections defined by Beal et al. (2015) and Ponsoni et al. (2016) for each of our simulations. These sections are illustrated in Fig. 7. Cross-sections of the mean EMC current (Fig. 7a,b) shows that although the mean transport of the EMC has increased from 24.6 Sv to 45.6 Sv in TOPO-BRIDGE, the shape of its vertical structure was not significantly impacted. The mean current velocity increases for the EMC from a maximum of 0.82 m s$^{-1}$ for REF to 1.37 m s$^{-1}$ for TOPO-BRIDGE.

For the AC (Fig. 7d,e), the maximum current is located 26 km offshore for REF and 39 km for TOPO-BRIDGE and is attenuated from 1.36 m s$^{-1}$ to 1.19 m s$^{-1}$. This is consistent with the findings of Beal and Elipot (2016) who showed a recent widening of the Agulhas Current related to an increase in mesoscale turbulence in the context of climate change.

### 3.2. Water masses and heat content

Fig. 8 shows Sea Surface Temperature (SST, panel a) and Salinity (SSS, panel c) of the reference simulation and the SST and SSS differences between TOPO-BRIDGE and REF (panels b and d). Temperature and salinity anomalies appear to be fairly anti-correlated, except in the Southern Ocean.

Significant anomalies of about −1.2 °C for SST and 0.5 PSU for SSS are perceptible in the central Mozambique Channel, South of Davie Ridge. The origin of these anomalies could be explained by the cut-off of the NMC which brings warmer water from lower latitudes in the form of TSW and RSW in the reference simulation. Fig. 5a shows that the contours underlying the NMC approach the equator up to 10° S, bringing heat into the channel. Once the channel is blocked, an absence of heat input in the Southern part of the channel may explain the negative SST anomaly (Fig. 5b) in the Mozambique Basin. This anomaly follows the inshore part of the AC to then dissipate in the South Atlantic. Similarly, a cut-off of the fresher water sources from lower latitudes can result in a positive SSS anomaly in the channel (Fig. 5a).

Once the channel is closed, a stronger EMC results in an increase in heat and freshwater input from the SEC into the southwest Indian subgyre, south of Madagascar. This may explain the warm and fresh anomalies in the region delimited by Madagascar, the Agulhas Current and the ARC (Fig. 5b,d).

Note that the colder and saltier anomalies originating from the central Mozambique Channel follow the inshore section of the Agulhas Current and propagate into the South Atlantic, affecting the Agulhas Leakage (Beal et al., 2011). By contrast, warmer and fresher anomalies originating from South Madagascar remain confined offshore of the Agulhas Current, in the southwest Indian subgyre. This corroborates the existence of a lateral mixing barrier for surface and thermocline waters in the Agulhas Current (Beal et al., 2006). As a consequence, this results in contrasting influences of the sources of the Agulhas Current on global ocean circulation: waters from the Mozambique Channel affect the Agulhas Leakage, whereas waters from the south of Madagascar are confined to the southwest Indian subgyre.
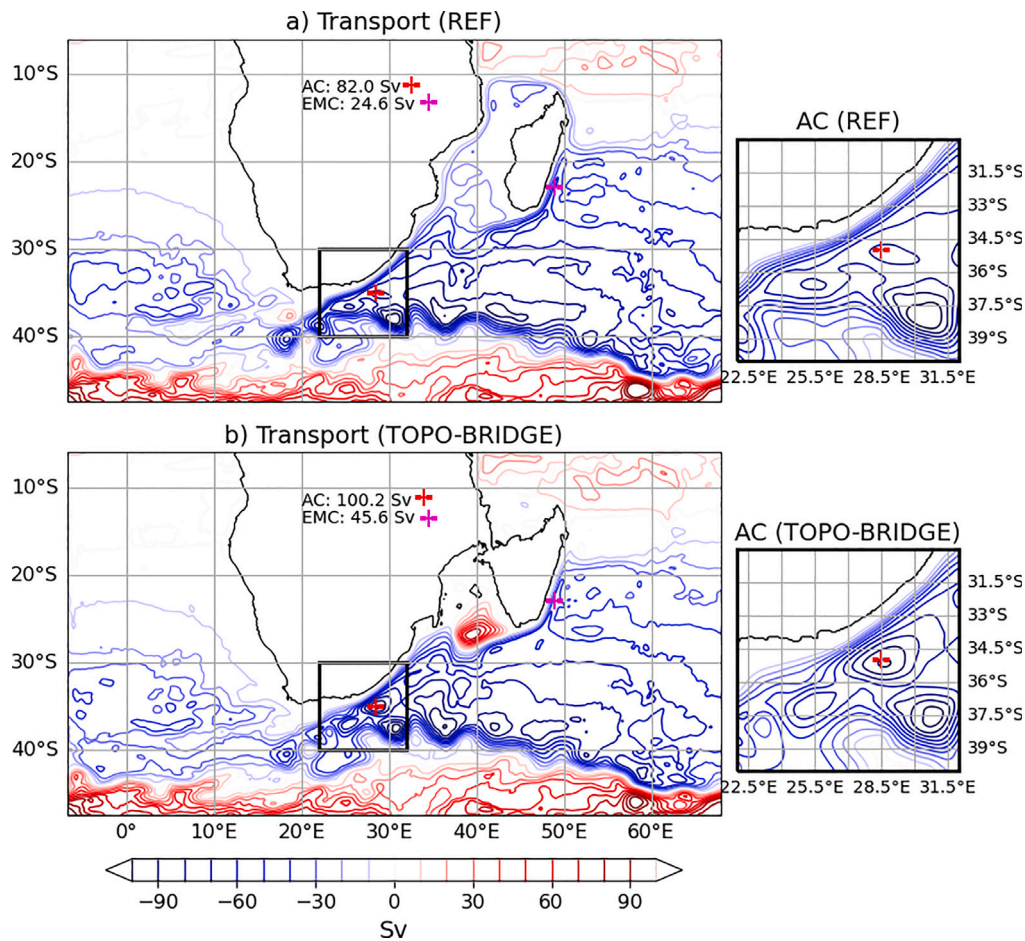
change. To understand these changes we look at how the closure of the Mozambique Channel affects geostrophic turbulence in the region.

Fig. 6 presents TOPO-BRIDGE RMS SSH (Fig. 6a) and its difference with REF (Fig. 6b). Turbulence due to mesoscale eddies from the north of the channel in the reference simulation completely collapses once the channel is closed (blue area south of Davie Ridge in Fig. 6b). However, south of the Mozambique Channel, southwest of Madagascar, RMS SSH more than doubles in the TOPO-BRIDGE simulation. This maximum is located in the eddy dipole generation region described by de Ruijter et al. (2004). The enhanced recirculation associated with a stronger EMC observed on Fig. 5b may be a signature of a mean flow rectification by this increased mesoscale eddy variability. Looking at

**Fig. 5.** Vertically integrated transport streamfunction (Transport) averaged over 2008–2017 for (a) the reference experiment REF and (b) for the modified bathymetry TOPO-BRIDGE (CI 10 Sv). Note the strong recirculation gyre South of the Mozambique Channel in the latter case. Right panels shows a zoom of the circulation in the Agulhas region (black rectangles on left panels).

*3.3. Bottom currents*

Because of their relevance for geophysical and sediment studies, we investigate how the Mozambique Channel closure impacts the mean bottom currents and their variability (Fig. 9). South of the Mozambique Channel, REF simulation (Fig. 9c) produces a weak mean bottom circulation following the isobaths in a cyclonic manner, in good agreement with previous literature (Miramontes et al., 2019). This average circulation increases significantly when the channel is blocked (Fig. 9a,c), especially southwest of Madagascar where acceleration can exceed 10 cm s$^{-1}$. This is significant as the currents in the region are initially in the order of 5 cm s$^{-1}$. Fig. 9d reveals the signature of a strong mean bottom current in the Mozambique basin which is redirected towards the South by remaining along the west side of Madagascar Ridge. This results in an increase of more than 10 cm s$^{-1}$ along the Mozambique Ridge (26° S, 38° E). The variability of bottom currents is also affected in the Mozambique basin with anomalies reaching 5 cm s$^{-1}$ (Fig. 9b).

**4. Discussion and conclusion**

By blocking the Mozambique Channel in an idealized numerical experiment, we have illustrated its importance for the southwest Indian Ocean. It results in a strengthening of the EMC and the formation of a recirculation gyre southwest of Madagascar. The increase in mesoscale turbulence induces a widening of the Agulhas Current. Cooler and saltier surface waters generated in the Mozambique channel propagate with the Agulhas Current towards the South Atlantic, while warmer and fresher waters from the South of Madagascar are confined in the

southwest Indian subgyre. Bottom circulation accelerates significantly in the Madagascar Basin.

South West Indian western boundary currents compensate a Sverdrup transport in addition to the Indonesian Throughflow (~ 10 Sv) and an Indian thermohaline circulation of about 10 Sv (Bryden et al., 2005; Casal et al., 2009). By blocking the Mozambique channel, the water that initially passed through it reinforces the EMC transport to attain 45.6 Sv. This strengthening occurs without change in the vertical structure of the current and with a decrease in turbulence along the east and south coasts of Madagascar. By analogy with the Agulhas Current, the steep slopes and the strength of the EMC current should fit the more stable regime applied for the northern Agulhas Current (Paldor and Lutjeharms, 2009).

Although the energy received by the basins should be almost equivalent in both simulations (this can be seen on time series of domain averaged kinetic energy, not shown), TOPO-BRIDGE has reached a new equilibrium with a higher level of surface eddy kinetic energy in the AC (as seen on Fig. 6), but a lower mean surface current (but wider as seen on Fig. 7). This is consistent with the process described by Beal and Elipot (2016). There is a significant increase in surface eddy variability in the Mozambique Basin. The detachment of the southward extension of the EMC from the southern tip of Madagascar causes the generation of cyclones, anticyclones and eddy dipoles, with the cyclones inshore and the anticyclones offshore (de Ruijter et al., 2004). In rotating tank experiments, in the case of a current meeting an obstacle to the right (corresponding to the EMC for the Southern Hemisphere), Boyer et al. (1987) have shown the correlation between an increase in the Rossby number and the amplification in the formation of cyclonic
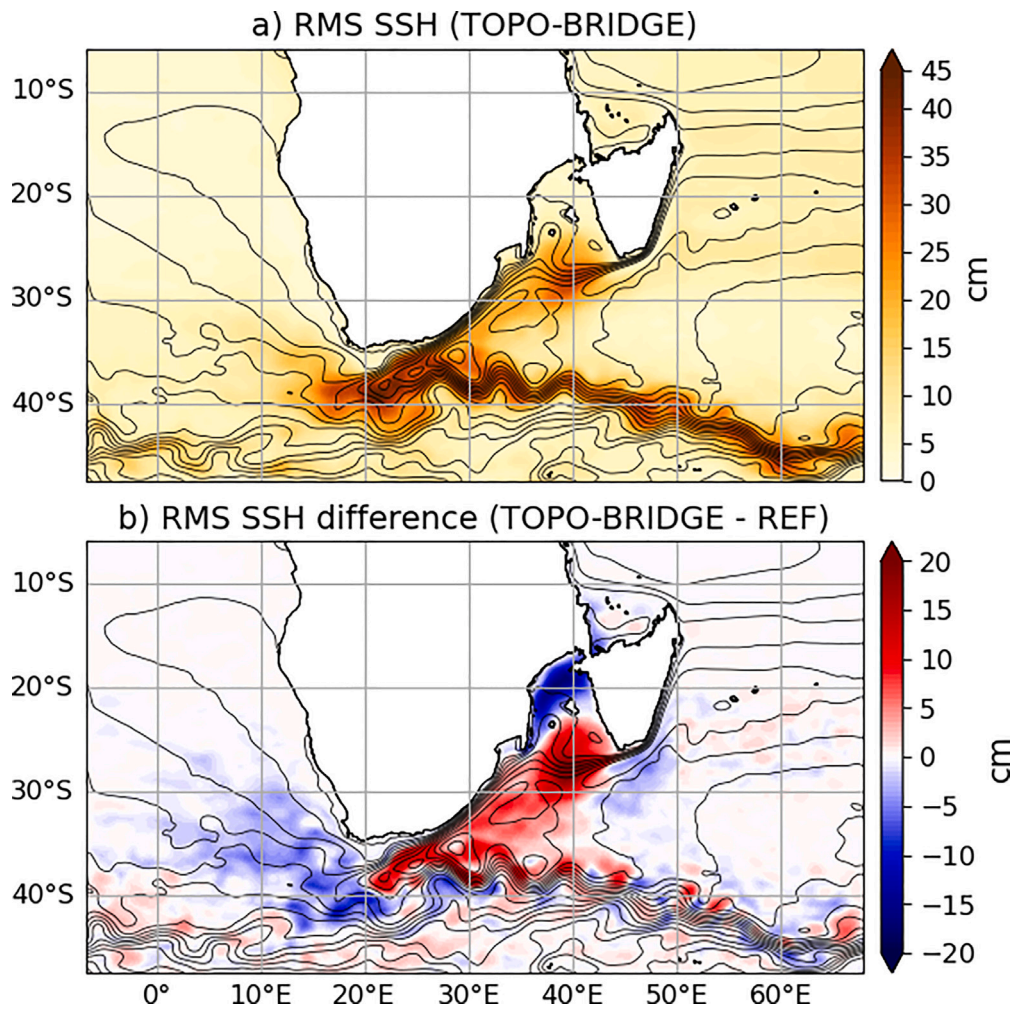
**Fig. 6.** (a) Root mean square of sea surface height (RMS SSH, in color) computed between 2008–2017 from daily values for TOPO-BRIDGE experiment. (b) RMS SSH difference between TOPO-BRIDGE and REF. Contours indicate the mean SSH (CI 10 cm).

eddies. This corresponds to the cyclonic eddy generation mode for the EMC extension exposed by Siedler et al. (2009) and to the cyclonic eddy generation process described by Penven et al. (2001) for the southern Agulhas Current. The rectification associated with the increase in cyclones in the northern part of the EMC extension could explain the large mean cyclonic recirculation seen downstream of Madagascar, as the mean-eddy energy transfer is predominately negative here (Halo et al., 2014b).

Significant changes in EMC strength and mesoscale variability southwest of Madagascar appear to have also resulted in an increase in cyclonic bottom circulation. As described above, increased mesoscale variability from the EMC detachment shows a signature in the form of a cyclonic recirculation in the mean vertically integrated transport. Eddy energy cascades can result in an energy transfer to the barotropic mode (Fu and Flierl, 1980; Smith and Vallis, 2001). This can be caused by eddy-eddy interactions in presence of stratification (Fu and Flierl, 1980; Smith and Vallis, 2001) and/or by eddy-topography interactions (Tedesco et al., 2022). Tedesco et al. (2022) have revealed the existence of such cascades in the Agulhas Retroflection region. An increase in barotropic transport should result in a stronger bottom circulation.

Anticyclones generated offshore the EMC and circulating in the southwest Indian subgyre were observed by de Ruijter et al. (2004). In TOPO-BRIDGE, they are of greater intensity and affect the SSH variability throughout the subgyre. From a long term mooring section, Beal and Elipot (2016) revealed a widening of the Agulhas Current over

time. This was explained by a recent increase in eddy variability. The wider Agulhas Current in presence of higher mesoscale turbulence seen in TOPO-BRIDGE is consistent with this finding.

de Ruijter et al. (2004) also shows that the increase in variability within the sub-gyre and the formation of dipoles moving towards the Southeast African coast can lead to early retroflection events (as occurred in 2001). By taking a closer look at the retroflection in terms of transport (Fig. 5), it appears that it occurs approximately 2° earlier (further east) in average in the TOPO-BRIDGE configuration. This could explain the decrease in variability in the Cape Basin observed in the TOPO-BRIDGE experiment. van Aken et al. (2013) and Russo et al. (2021) link early retroflection events to the formation of Natal pulses following the inshore part of the Agulhas current which may short-circuit the retroflection. The increase in Natal pulses activity in the TOPO-BRIDGE experiment is visible in SSH animations (available as supplementary material). The position of the retroflection may impact the Agulhas leakage (Dencausse et al., 2010b,a), with possible implications for the Atlantic overturning circulation (Beal et al., 2011). The limited extension of our model grids prevents us from addressing these possible consequences in our regional simulations. This is one of the principal limits of our approach.

The consequences of the closing of the Mozambique Channel in TOPO-BRIDGE are also clear in the water mass properties. The closing of the fluxes from lower latitudes results in colder and saltier surface waters in the central Mozambique Channel. By contrast, EMC strengthening results in warmer and fresher waters, feeding the southwest
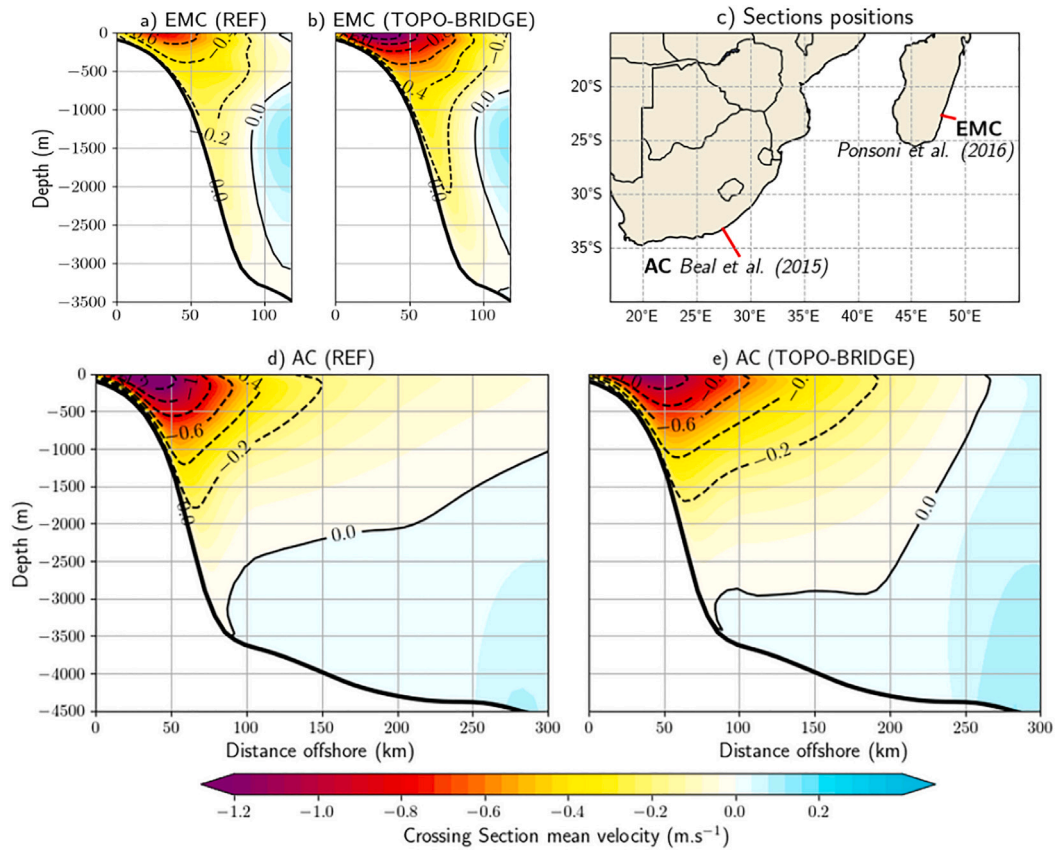
**Fig. 7.** Mean velocities orthogonal to the EMC and AC sections defined by Ponsoni et al. (2016) and Beal et al. (2015) averaged over 2008–2017, for the REF (left) and for TOPO-BRIDGE (right). (CI 20 cm s$^{-1}$, solid northward, dashed southward).
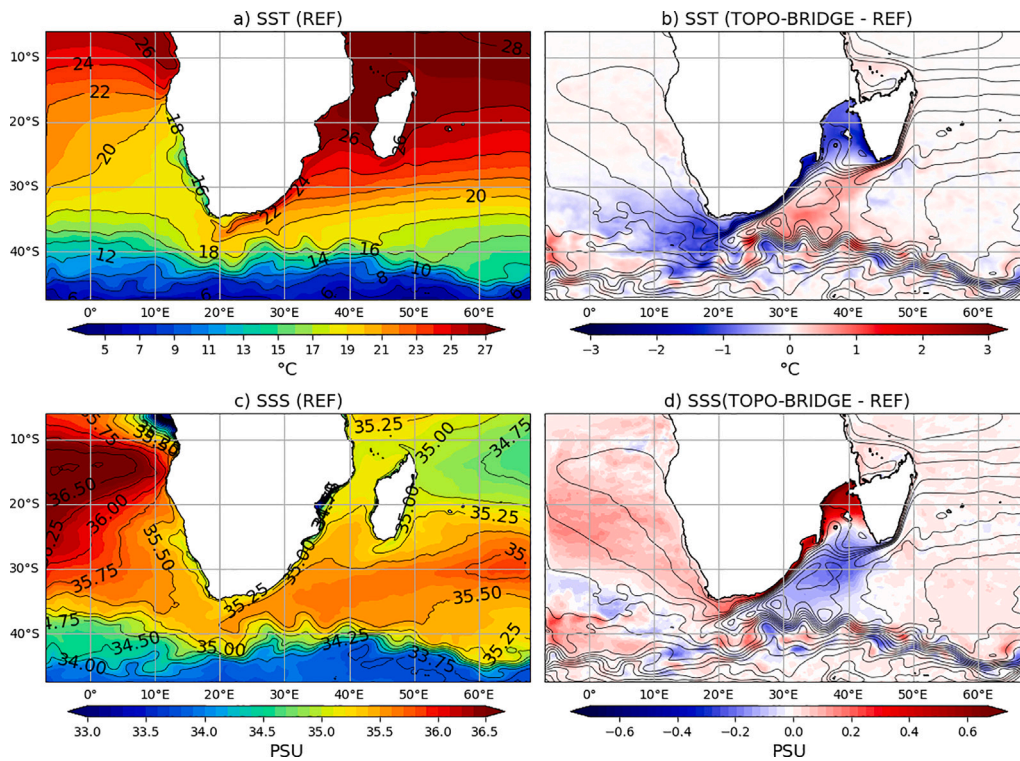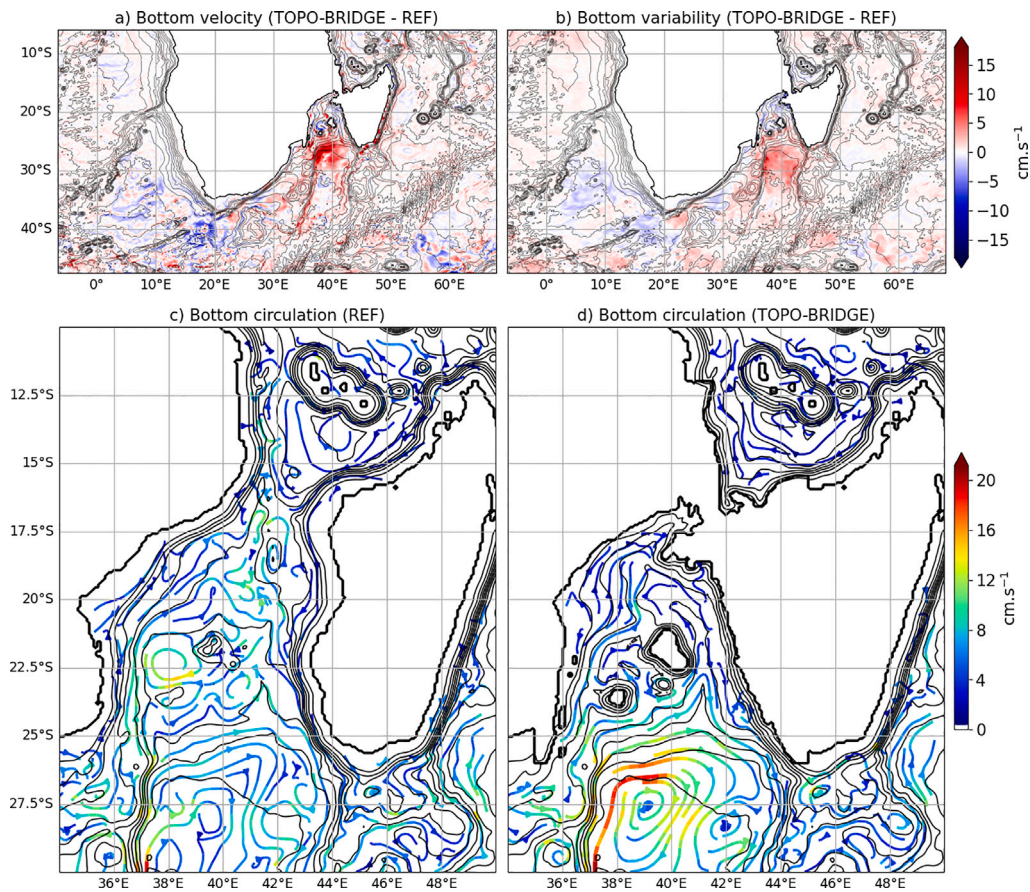


**Fig. 8.** (a) SST and (c) SSS averaged over 2008–2017 for the reference experiment (respectively CI = 2 °C and CI = 0.25 PSU). (b) SST and (d) SSS difference between the experiment with modified bathymetry and the reference experiment averaged over 2008–2017, contours indicate the mean SSH (CI = 10 cm).

**Fig. 9.** (a) Differences in mean bottom velocities for the period 2008–2017 between TOPO-BRIDGE and REF. (b) Differences in bottom current variability ($\sqrt{EKE}$). Mean bottom circulation for REF (c) and TOPO-BRIDGE (d) simulations. Black contours indicate the bathymetry (CI 500 m).

Indian subgyre from the south of Madagascar. This contrast in anomalies is separated by the Agulhas Current, acting as a barrier for lateral mixing (Beal et al., 2006). The anomalies generated in the Mozambique Channel can propagate into the South Atlantic, participating in the Agulhas Leakage (Beal et al., 2011).

Although motivated by past topography considerations (McCall, 1997; Pellen et al., 2022), TOPO-BRIDGE configuration can be identified as a sensitivity analysis for regional circulation over a different bathymetry, in the same way as Penven et al. (2006) investigated the consequences of removing Madagascar on the Agulhas western boundary current. As such, it is a geophysical fluid dynamics study, and cannot be considered as a paleoclimatic experiment because the large scale boundary conditions and the atmospheric forcing remain unchanged here. These are the main limitations of our experimental system to address past conditions. For example, the atmospheric forcing does not adapt to the new configuration and the sensible heat flux tends to reduce the SST to the temperature values prescribed by ERA5. Large scale conditions would also have been different in the past climate. This introduces one of the perspectives of improvement of the TOPO-BRIDGE configuration. Zhang et al. (2020) studied the Eocene period in a coupled IPSL simulation at 2° resolution. Inserting a high-resolution regional coupled ocean-atmosphere model into a 2° global model would allow for a true paleoclimate simulation while remaining locally at a mesoscale resolution. This could allow us to study how changes in the leakage (saltier and colder) would influence the rest of the global climate and circulation and consider their possible feedbacks with the Agulhas current system.

The way in which the addition of a continental bridge between Madagascar and Africa has modified the region's circulation in a current and regional configuration incites us to work on a reconstruction of circulation 35 million years ago. This could be achieved by repositioning the continents and working in a coupled global ocean-atmosphere simulation. If the relative position between Africa and Madagascar has not changed for 120 million years (Reeves, 2014), then, 35 million years ago, Africa would have been much further south than today, which would directly modify the Coriolis term as well as the position of Madagascar in relation to the subtropical gyre and the surrounding mean winds. Foraminifera studies, lithologies changes (e.g. sortable silt mean size) would make it possible to compare these results with observations in existing drilling sites and cores (Haynes, 1981; Wu et al., 2019). Bottom current changes could also leave their imprints in sediment in the form of changing contourites drifts geometries (Rebesco and Camerlenghi, 2008) as can their combination with eddies (Babonneau et al., 2022).

## CRediT authorship contribution statement

**Théo Le Hir:** Conceptualization, Data curation, Formal analysis, Methodology, Validation, Visualization, Writing – original draft, review & editing. **Pierrick Penven:** Conceptualization, Funding acquisition, Methodology, Software, Supervision, Validation, Visualization, Writing – original draft, review & editing. **Thierry Huck:** Conceptualization, Methodology, Supervision, Writing – original draft, review & editing. **Romain Pellen:** Data curation, Methodology, Resources, Supervision, Writing – original draft, review & editing. **Maryline Moulin:** Conceptualization, Funding acquisition, Methodology, Supervision, Validation, Writing – original draft, review & editing. **Marina Rabineau:** Conceptualization, Methodology, Resources, Validation, Writing – original draft, review & editing. **Daniel Aslanian:** Conceptualization, Funding acquisition, Methodology, Resources, Supervision, Validation, Writing – original draft, review & editing.

## Declaration of competing interest

The authors declare that they have no known competing financial interests or personal relationships that could have appeared to influence the work reported in this paper.

## Acknowledgments

## Appendix A. Supplementary data

Supplementary material related to this article can be found online at https://doi.org/10.1016/j.jmarsys.2024.104024.

## Data availability

The model used is the Coastal and Regional Ocean COmmunity model (CROCO, freely available from https://www.croco-ocean.org/) (Auclair et al., 2022). The SouthWest indiAn subtropical Gyre (SWAG12) configuration has been created using scripts from CROCO-TOOLS (freely available from https://www.croco-ocean.org) (Penven et al., 2008, 2022). SWAG12 model outputs are freely available from the IPSL Thredds server: https://thredds-su.ipsl.fr/thredds/catalog/idris_thredds/work/ryff001/RUN_SWAG12/AVG/catalog.html.

## References

Auclair, F., Benshila, R., Bordois, L., Boutet, M., Brémond, M., Caillaud, M., Cambon, G., Capet, X., Debreu, L., Ducousso, N., Dufois, F., Dumas, F., Ethé, C., Gula, J., Hourdin, C., Illig, S., Jullien, S., Corre, M.L., Gac, S.L., Gentil, S.L., Lemarié, F., Marchesiello, P., Mazoyer, C., Morvan, G., Nguyen, C., Penven, P., Person, R., Pianezze, J., Pous, S., Renault, L., Roblou, L., Sepulveda, A., Theetten, S., 2022. Coastal and Regional Ocean COmmunity model (1.3). Zenodo, http://dx.doi.org/10.5281/zenodo.7415343.

Babonneau, N., Raisson, F., Genêt, A., Lopes, U., Fierens, R., Miramontes, E., Révillon, S., Rabineau, M., Droz, L., Belleney, D., Moulin, M., Aslanian, D., 2022. Contourite on the Limpopo Corridor, Mozambique margin: long-term evolution, facies distribution and Quaternary processes. Sedimentology 70, 728–758. http://dx.doi.org/10.1111/sed.13045.

Beal, L.M., Chereskin, T.K., Lenn, Y.D., Elipot, S., 2006. The sources and mixing characteristics of the Agulhas current. J. Phys. Oceanogr. 36, 2060–2074. http://dx.doi.org/10.1175/JPO2964.1.

Beal, L.M., De Ruijter, W.P., Biastoch, A., Zahn, R., 2011. On the role of the Agulhas system in ocean circulation and climate. Nature 472 (7344), 429–436. http://dx.doi.org/10.1038/nature09983.

Beal, L.M., Elipot, S., 2016. Broadening not strengthening of the Agulhas Current since the early 1990s. Nature 540 (7634), 570–573. http://dx.doi.org/10.1038/nature19853.

Beal, L.M., Elipot, S., Houk, A., Leber, G.M., 2015. Capturing the transport variability of a western boundary jet: Results from the Agulhas Current Time-Series Experiment (ACT). J. Phys. Oceanogr. 45 (5), 1302–1324. http://dx.doi.org/10.1175/JPO-D-14-0119.1.

Beckmann, A., Haidvogel, D., 1993. Numerical simulation of flow around a tall isolated seamount. Part I: Problem formulation and model accuracy. J. Phys. Oceanogr. 23, 1736–1753. http://dx.doi.org/10.1175/1520-0485(1993)023<1736:NSOFAA>2.0.CO;2.

Boyer, D.L., Chen, R., D'Hieres, G.C., Didelle, H., 1987. On the formation and shedding of vortices from side-wall mounted obstacles in rotating systems. Dyn. Atmospheres Oceans 11 (1), 59–86. http://dx.doi.org/10.1016/0377-0265(87)90014-5.

Bryden, H.L., Beal, L.M., Duncan, L.M., 2005. Structure and transport of the Agulhas Current and its temporal variability. J. Oceanogr. 61, 479–492. http://dx.doi.org/10.1007/s10872-005-0057-8.

Casal, T.G.D., Beal, L.M., Lumpkin, R., Johns, W.E., 2009. Structure and downstream evolution of the Agulhas Current system during a quasi-synoptic survey in February - March 2003. J. Geophys. Res. 114, C03001. http://dx.doi.org/10.1029/2008JC004954.

Chapman, P., Di Marco, S., Davis, R., Coward, A., 2003. Flow at intermediate depths around madagascar based on ALACE float trajectories. Deep Sea Res. II: Topical Stud. Oceanogr. 50 (12–13), 1957–1986. http://dx.doi.org/10.1016/S0967-0645(03)00040-7.

Charles, C., Pelleter, E., Révillon, S., Nonnotte, P., Jorry, S.J., Kluska, J.-M., 2020. Intermediate and deep ocean current circulation in the Mozambique Channel: New insights from ferromanganese crust Nd isotopes. Mar. Geol. 430, 106356. http://dx.doi.org/10.1016/j.margeo.2020.106356.

de Ruijter, W.P., van Aken, H.M., Beier, E.J., Lutjeharms, J.R., Matano, R.P., Schouten, M.W., 2004. Eddies and dipoles around South Madagascar: formation, pathways and large-scale impact. Deep Sea Res. II: Topical Stud. Oceanogr. 51 (3), 383–400. http://dx.doi.org/10.1016/j.dsr.2003.10.011.

Dencausse, G., Arhan, M., Speich, S., 2010a. Routes of Agulhas rings in the southeastern Cape Basin. Deep Sea Res. II: Topical Stud. Oceanogr. 57 (11), 1406–1421. http://dx.doi.org/10.1016/j.dsr.2010.07.008.

Dencausse, G., Arhan, M., Speich, S., 2010b. Spatio-temporal characteristics of the Agulhas Current retroflection. Deep Sea Res. II: Topical Stud. Oceanogr. 57 (11), 1392–1405. http://dx.doi.org/10.1016/j.dsr.2010.07.004.

Fu, L.L., Flierl, G.R., 1980. Nonlinear energy and enstrophy transfers in a realistically stratified ocean. Dyn. Atmos. Oceans 4, 219–246.

GEBCO Bathymetric Compilation Group, 2020. The GEBCO 2020 Grid - a continuous terrain model of the global oceans and land. British Oceanographic Data Centre, National Oceanography Centre, NERC, UK, http://dx.doi.org/10.5285/a29c5465-b138-234d-e053-6c86abc040b9.

Génin, F., Mazza, P.P.A., Pellen, R., Rabineau, M., Aslanian, D., Masters, J.C., 2022. Co-evolution assists geographic dispersal: the case of Madagascar. Biol. J. Linnean Soc. 137 (2), 163–182. http://dx.doi.org/10.1093/biolinnean/blac090.

Halo, I., Backeberg, B., Penven, P., Ansorge, I., Reason, C., Ullgren, J., 2014a. Eddy properties in the Mozambique Channel: A comparison between observations and two numerical ocean circulation models. Deep Sea Res. II: Topical Stud. Oceanogr. 100, 38–53. http://dx.doi.org/10.1016/j.dsr2.2013.10.015.

Halo, I., Penven, P., Backeberg, B., Ansorge, I., Shillington, F., Roman, R., 2014b. Mesoscale eddy variability in the southern extension of the East Madagascar Current: Seasonal cycle, energy conversion terms, and eddy mean properties. J. Geophys. Res. 119, 7324–7356. http://dx.doi.org/10.1002/2014JC009820.

Haynes, J.R., 1981. Foraminifera. Springer.

Hersbach, H., Bell, B., Berrisford, P., Hirahara, S., Horányi, A., Muñoz-Sabater, J., Nicolas, J., Peubey, C., Radu, R., Schepers, D., 2020. The ERA5 global reanalysis. Q. J. R. Meteorol. Soc. 146 (730), 1999–2049. http://dx.doi.org/10.1002/qj.3803.

Lellouche, J.-M., Greiner, E., Le Galloudec, O., Garric, G., Regnier, C., Drevillon, M., Benkiran, M., Testut, C.-E., Bourdalle-Badie, R., Gasparin, F., 2018. Recent updates to the copernicus marine service global ocean monitoring and forecasting real-time 1/12° high-resolution system. Ocean Sci. 14, 1093–1126. http://dx.doi.org/10.5194/os-14-1093-2018.

Locarnini, M., Mishonov, A., Baranova, O., Boyer, T., Zweng, M., Garcia, H., Seidov, D., Weathers, K., Paver, C., Smolyar, I., 2018. World Ocean Atlas 2018, Volume 1: Temperature. Technical Report., NOAA Atlas NESDIS 81, 52pp, National Centers for Environmental Information, Silver Spring, MD, USA.

Lopes, U., Babonneau, N., Fierens, R., Revillon, S., Raisson, F., Miramontes, E., Rabineau, M., Aslanian, D., Moulin, M., 2023. Foraminiferal sandy contourite of the Limpopo Corridor (Mozambique margin): Facies characterization and paleoceanographic record. Mar. Geol. 459, 107031. http://dx.doi.org/10.1016/j.margeo.2023.107031.

Lutjeharms, J.R.E., 2006. The Agulhas Current. Springer-Verlag.

Lutjeharms, J.R.E., Ansorge, I.J., 2001. The Agulhas return current. J. Mar. Syst. 30 (1–2), 115–138. http://dx.doi.org/10.1016/S0924-7963(01)00041-0.

Lutjeharms, J.R.E., Bang, N.D., Duncan, C.P., 1981. Characteristics of the currents east and south of Madagascar. Deep Sea Res A. Oceanogr. Res. Pap. 28 (9), 879–899.

Masters, J.C., Génin, F., Zhang, Y., Pellen, R., Huck, T., Mazza, P.P., Rabineau, M., Doucouré, M., Aslanian, D., 2021. Biogeographic mechanisms involved in the colonization of Madagascar by African vertebrates: Rifting, rafting and runways. J. Biogeogr. 48 (3), 492–510. http://dx.doi.org/10.1111/jbi.14032.

Mazza, P.P.A., Buccianti, A., Savorelli, A., 2019. Grasping at straws: A re-evaluation of sweepstakes colonisation of islands by mammals. Biol. Rev. 94, 1364–1380. http://dx.doi.org/10.1111/brv.12506.

McCall, R.A., 1997. Implications of recent geological investigations of the Mozambique Channel for the mammalian colonization of Madagascar. Proc. Royal Soc. London B 264, 663–665. http://dx.doi.org/10.1098/rspb.1997.0094.

Miramontes, E., Penven, P., Fierens, R., Droz, L., Toucanne, S., Jorry, S.J., Jouet, G., Pastor, L., Jacinto, R.S., Gaillot, A., 2019. The influence of bottom currents on the Zambezi Valley morphology (Mozambique Channel, SW Indian ocean): In situ current observations and hydrodynamic modelling. Mar. Geol. 410, 42–55. http://dx.doi.org/10.1016/j.margeo.2019.01.002.

Paldor, N., Lutjeharms, J.R.E., 2009. Why is the stability of the Agulhas Current geographically bi-modal? Geophys. Res. Lett. 36, L14604. http://dx.doi.org/10.1029/2009GL038445.

Pellen, R., Aslanian, D., Rabineau, M., 2022. Reconstruction of land-sea DTMs at several geological periods: Example of the Mozambique Channel and Madagascar. http://dx.doi.org/10.17882/89892, SEANOE.

Penven, P., Cambon, G., Marchesiello, P., Sepulveda, A., Benshila, R., Illig, S., Jullien, S., Corre, M.L., Gentil, S.L., Morvan, G., 2022. CROCO tools (1.3). Zenodo, http://dx.doi.org/10.5281/zenodo.7432028.

Penven, P., Lutjeharms, J., Florenchie, P., 2006. Madagascar: A pacemaker for the Agulhas Current system? Geophys. Res. Lett. 33 (17), L17609. http://dx.doi.org/10.1029/2006GL026854.

Penven, P., Lutjeharms, J.R.E., Marchesiello, P., Roy, C., Weeks, S.J., 2001. Generation of cyclonic eddies by the Agulhas Current in the lee of the Agulhas Bank. Geophys. Res. Lett. 28, 1055–1058. http://dx.doi.org/10.1029/2000GL011760.

Penven, P., Marchesiello, P., Debreu, L., Lefèvre, J., 2008. Software tools for pre- and post-processing of oceanic regional simulations. Env. Model. Soft. 23, 660–662. http://dx.doi.org/10.1016/j.envsoft.2007.07.004.

Ponsoni, L., Aguiar-González, B., Ridderinkhof, H., Maas, L.R., 2016. The East Madagascar Current: Volume transport and variability based on long-term observations. J. Phys. Oceanogr. 46 (4), 1045–1065. http://dx.doi.org/10.1175/JPO-D-15-0154.1.

Rebesco, M., Camerlenghi, A., 2008. Developments in sedimentology. In: Contourites, vol. 60, Elsevier, Amsterdam, The Netherlands, pp. 1–663.

Reeves, C., 2014. The position of Madagascar within Gondwana and its movements during Gondwana dispersal. J. Afr. Earth Sci. 94, 45–57. http://dx.doi.org/10.1016/j.jafrearsci.2013.07.011.

Richardson, P.L., 2007. Agulhas leakage into the Atlantic estimated with subsurface floats and surface drifters. Deep Sea Res., Part I 54, 1361–1389. http://dx.doi.org/10.1016/j.dsr.2007.04.010.

Ridderinkhof, H., van der Werf, P.M., Ullgren, J.E., van Aken, H.M., van Leeuwen, P.J., de Ruijter, W.P.M., 2010. Seasonal and interannual variability in the Mozambique Channel from moored current observations. J. Geophys. Res. 115, C06010. http://dx.doi.org/10.1029/2009JC005619.

Russo, C.S., Lamont, T., Krug, M., 2021. Spatial and temporal variability of the Agulhas Retroflection: Observations from a new objective detection method. Remote Sens. Environ. 253 (4), 112239. http://dx.doi.org/10.1016/j.rse.2020.112239.

Schott, F.A., McCreary, J.P., 2001. The monsoon circulation of the Indian ocean. Prog. Oceanogr. 51 (1), 1–123. http://dx.doi.org/10.1016/S0079-6611(01)00083-0.

Shchepetkin, A., McWilliams, J.C., 2005. The Regional Oceanic Modeling System: A split-explicit, free-surface, topography-following-coordinate ocean model. Ocean Model. 9, 347–404.

Siedler, G., Rouault, M., Biastoch, A., Backeberg, B., Reason, C.J.C., Lutjeharms, J.R.E., 2009. Modes of the southern extension of the East Madagascar Current. J. Geophys. Res. 114, C01005. http://dx.doi.org/10.1029/2008JC004921.

Simpson, G.G., 1940. Mammals and land bridges. J. Wash. Acad. Sci. 30 (4), 137–163.

Smith, K., Vallis, G., 2001. The scales and equilibration of midocean eddies: Freely evolving flow. J. Phys. Oceanogr. 31, 554–571. http://dx.doi.org/10.1175/1520-0485(2001)031<0554:TSAEOM>2.0.CO;2.

Speich, S., Lutjeharms, J.R.E., Penven, P., Blanke, B., 2006. Role of bathymetry in Agulhas Current configuration and behaviour. Geophys. Res. Lett. 33, L23611. http://dx.doi.org/10.1029/2006GL027157.

Taburet, G., Sanchez-Roman, A., Ballarotta, M., Pujol, M.-I., Legeais, J.-F., Fournier, F., Faugere, Y., Dibarboure, G., 2019. DUACS DT2018: 25 years of reprocessed sea level altimetry products. Ocean Sci. 15 (5), 1207–1224. http://dx.doi.org/10.5194/os-15-1207-2019.

Tedesco, P., Gula, J., Ménesguen, C., Penven, P., Krug, M.J., 2019. Generation of submesoscale frontal eddies in the Agulhas Current. J. Geophys. Res. 124, 7606–7625. http://dx.doi.org/10.1029/2019JC015229.

Tedesco, P., Gula, J., Penven, P., Ménesguen, C., 2022. Mesoscale eddy kinetic energy budgets and transfers between vertical modes in the Agulhas Current. J. Phys. Oceanogr. 52, 677–704. http://dx.doi.org/10.1175/JPO-D-21-0110.1.

Tomczak, M., Godfrey, J.S., 1994. Regional Oceanography: An Introduction, first ed. Pergamon.

van Aken, H., Lutjeharms, J., Rouault, M., Whittle, C., de Ruijter, W., 2013. Observations of an early Agulhas current retroflection event in 2001: A temporary cessation of inter-ocean exchange south of Africa? Deep Sea Res. II: Topical Stud. Oceanogr. 72, 1–8. http://dx.doi.org/10.1016/j.dsr.2012.11.002.

van der Werf, P.M., van Leeuwen, P.J., Ridderinkhof, H., de Ruijter, W.P.M., 2010. Comparison between observations and models of the Mozambique Channel transport: Seasonal cycle and eddy frequencies. J. Geophys. Res. 115, C02002. http://dx.doi.org/10.1029/2009JC005633.

Voldsund, A., Aguiar-González, B., Gammelsrød, T., Krakstad, J.-O., Ullgren, J., 2017. Observations of the East Madagascar Current system: Dynamics and volume transports. J. Mar. Res. 75, 531–555. http://dx.doi.org/10.1357/002224017821836725.

Weatherall, P., Marks, K.M., Jakobsson, M., Schmitt, T., Tani, S., Arndt, J.E., Rovere, M., Chayes, D., Ferrini, V., Wigley, R., 2015. A new digital bathymetric model of the world's oceans. Earth Space Sci. 2 (8), 331–345. http://dx.doi.org/10.1002/2015EA000107.

Wu, S., Kuhn, G., Diekmann, B., Lembke-Jene, L., Tiedemann, R., Zheng, X., Ehrhardt, S., Arz, H.W., Lamy, F., 2019. Surface sediment characteristics related to provenance and ocean circulation in the Drake Passage sector of the Southern Ocean. Deep Sea Res., Part I 154, 103135. http://dx.doi.org/10.1016/j.dsr.2019.103135.

Zhang, Y., Huck, T., Lique, C., Donnadieu, Y., Ladant, J.-B., Rabineau, M., Aslanian, D., 2020. Early Eocene vigorous ocean overturning and its contribution to a warm Southern Ocean. Climate Past 16, 1263–1283. http://dx.doi.org/10.5194/cp-16-1263-2020.